CHEMISTRY

Palladium-catalyzed intermolecular asymmetric dearomatizative arylation of indoles and benzofurans

Yang Xi[1], Youzhi Xu[2], Linlin Fan[1], Chenchen Wang[1], Tingting Xia[1], Genping Huang[2]*, Jingping Qu[1], Yifeng Chen[1,3,4]*

Indoles represent one of the most robust and synthetically versatile classes of heteroaromatic compounds. However, the stereoselective conversion of planar indole rings into three-dimensional indoline skeletons bearing multiple stereogenic centers remains a persistent challenge in organic synthesis. Herein, we describe an intermolecular catalytic asymmetric dearomatization of simple indoles via a palladium-catalyzed three-component cross-coupling reaction. By using readily accessible diazonium salts and aromatic boronic acids as arylative reagents under a ligand-swap strategy, this method enables the efficient construction of 2,3-diarylated indolines. Mechanistic studies reveal that the chiral BiOx ligand governs the highly stereoselective migratory insertion of the aryl-palladium intermediate into the indole's C═C double bond with complete diastereo- and regioselectivity, whereas the achiral fumarate ligand facilitates the reductive elimination step, as corroborated by density functional theory calculations. Furthermore, this protocol is extended to the dearomatative diarylation of benzofurans, affording chiral 2,3-dihydrobenzofuran derivatives with high stereocontrol.

INTRODUCTION

Heterocycles are highly valuable structural motifs, as evidenced by their ubiquity in natural products and pharmaceuticals (*1*). Among aromatic nitrogen heterocycles, indoles and their derivatives have garnered sustained attention due to their prevalence in bioactive molecules (*2*). Developing novel strategies for selective indole functionalization remains a pivotal research focus in organic chemistry (*3*–*5*). Traditional approaches leverage indoles as electron-rich nucleophiles in electrophilic substitutions (*6*, *7*), whereas recent advances emphasize site-selective C─H functionalization and cross-coupling to incorporate functional groups (*8*, *9*) (Fig. 1A). A seminal work by Szmuszkovicz demonstrated indole dearomatization via Michael addition to generate indoline scaffolds (Fig. 1B, i) (*10*), inspiring subsequent efforts to construct three-dimensional indolines through C2─C3 π-bond cleavage (*11*–*13*). Catalytic asymmetric dearomative cyclization has emerged as a powerful route to fused or spiro indolines prevalent in alkaloids and drugs (*14*–*23*). However, the direct intermolecular conversion of simple indoles into 2,3-disubstituted indolines—enantioselectively installing two distinct groups at C2 and C3—remains elusive (*23*–*26*). Existing intermolecular catalytic asymmetric dearomatization (CADA) strategies, such as transition metal–catalyzed hydrogenation (*27*–*29*) or hydrofunctionalization (*30*, *31*), require prefunctionalization of indoles (Fig. 1B, ii). Ready elegantly disclosed 2-lithiated indole triggered stereoselective 1,2-boronate rearrangement to access multisubstituted indoline (*32*–*35*).

Substantial advances in palladium-catalyzed asymmetric dearomative cascade Heck reactions of indoles have enabled the construction of diverse fused indolines (*36*, *37*). The well-established mechanism for dearomative Heck reactions of indole-tethered aryl halides involves intramolecular *syn* migratory insertion, as elegantly demonstrated by Jia, You, Fukuyama, and Zhou (*38*–*52*). Notably, the You group recently reported the sole example of an intermolecular Pd-catalyzed dearomative Heck reaction using tetrahydrocyclopenta[*b*]indole and aryl iodide (*53*). Despite progress, achieving highly regio-, diastereo-, and stereoselective migratory insertion of one fragment into the indole's C2─C3 π-bond, followed by interception with an external fragment—specifically, intermolecular catalytic asymmetric three-component dearomative cross-coupling of simple indoles—remains a formidable challenge (*54*–*60*). Building on our recent ligand-swap strategy for palladium-catalyzed enantioselective difunctionalization of internal enamides and styrenes (*61*, *62*) and inspired by Ni-catalyzed 1,2-diarylation of unactivated alkenes with directing groups at remote positions of C═C double bonds (*63*–*72*), we sought to address the inherent inertness of the aromatic indole ring (Fig. 1C). Although indoles readily undergo Pd-catalyzed direct C─H arylation (*73*–*75*), their C═C double bond exhibits poor reactivity toward intermolecular migratory insertion of aryl-Pd(II) species, often favoring Suzuki cross-coupling between aryl boronic acids and diazonium salts. Regioselectivity in migratory insertion further complicates functionalization (*76*). Herein, we disclose the Pd-catalyzed asymmetric intermolecular diarylation of simple indoles using aromatic boronic acids and diazonium salts enabled by the ligand-swap strategy: A chiral ligand ensures stereoselective migratory insertion, whereas an achiral ligand promotes reductive elimination (*61*, *62*). This method delivers *cis*-2,3-diarylated indolines with complete regio- and diastereoselectivity and high enantioselectivity, even for substrates resistant to high-pressure asymmetric hydrogenation (*29*). The protocol also extends to benzofurans, enabling efficient synthesis of chiral 2,3-dihydrobenzofuran derivatives.

RESULTS AND DISCUSSION

Reaction optimization

We initiated our study by optimizing N-protected indole substrates (**1**) under conditions using 2.5 mol % $[Pd(allyl)Cl]_2$ as the catalyst, 10 mol % (*S*)-^{i}Pr-BiOx as the chiral ligand, 16 mol % dimethyl fumarate

[1]Key Laboratory for Advanced Materials and Joint International Research Laboratory of Precision Chemistry and Molecular Engineering, Feringa Nobel Prize Scientist Joint Research Center, Frontiers Science Center for Materiobiology and Dynamic Chemistry, School of Chemistry and Molecular Engineering, East China University of Science and Technology, Shanghai 200237, China. [2]Department of Chemistry, School of Science, Tianjin University, Tianjin 300072, China. [3]State Key Laboratory of Organometallic Chemistry, Shanghai Institute of Organic Chemistry, Chinese Academy of Sciences, Shanghai 200032, China. [4]School of Chemistry and Chemical Engineering, Henan Normal University, Xinxiang 453007, China.
*Corresponding author. Email: gphuang@tju.edu.cn (G.H.); yifengchen@ecust.edu.cn (Y.C.)

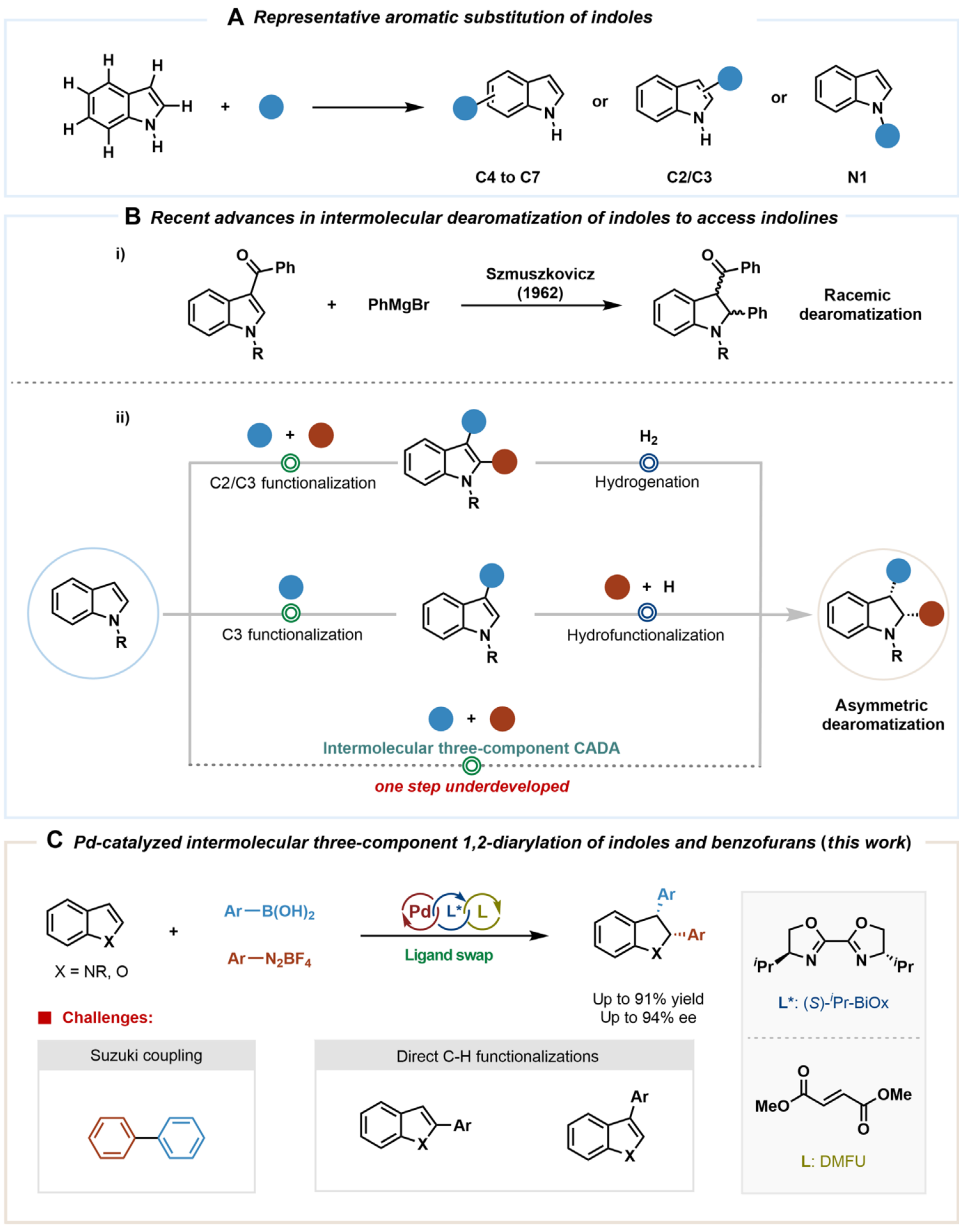

Fig. 1. Introduction of indole functionalization. (**A**) Classic transformation of indoles. (**B**) Recent advances in intermolecular dearomatization of indoles to access indolines. (**C**) This work: Pd-catalyzed intermolecular three-component 1,2-diarylation of indoles and benzofurans.

(DMFU), and 1.0 equiv Ag_2CO_3 as additives in *tert*-amyl alcohol at 20°C, using 4-$MeC_6H_4B(OH)_2$ (**2a**) and 4-$MeOC_6H_4N_2BF_4$ (**3a**) as coupling partners (Fig. 2, left). The N-Boc–protected indole (**1a**) delivered *cis*-2,3-diarylated product **4a** in 57% yield with 85:15 enantiomeric ratio (er), confirming regioselective migratory insertion at the indole's C-2 position to form a C-3–substituted benzylic palladium intermediate. Screening of N-protecting groups revealed that carbamates (e.g., **1b** and **1c**) offered no significant improvement, whereas N-Bz-indole (**1d**) markedly enhanced reactivity, achieving 91% yield and 91.5:8.5 er. Further optimization with a 3,5-bis(trifluoromethyl)benzoyl group (**1g**) provided **4g** in 77% yield and 94.5:5.5 er, outperforming other substituents [e.g., Ac, Ts, $P(O)^tBu_2$ (*77*), or Me groups; **1h** to **1l**]. Subsequent refinement of reaction conditions for **1g** (Fig. 2, right) demonstrated the necessity of DMFU (accelerating reductive elimination) (*78*–*82*) and Ag_2CO_3 (facilitating oxidative addition of diazonium salts). Adding 2.0 equiv H_2O slightly improved er (likely via enhanced diazonium solubility), although the yield remained moderate. Adjusting the concentration or temperature (15°C) proved ineffective, whereas reducing boronic acid stoichiometry (2.0 equiv) under final optimized conditions ($[Pd(allyl)Cl]_2$ (2.5 mol %), (*S*)-^{i}Pr-BiOx (10 mol %), DMFU (16 mol %), Ag_2CO_3 (2.0 equiv), H_2O (2.0 equiv), *tert*-amyl alcohol (0.2 M), 20°C) afforded **4g** as a single regio- and diastereomer in 80% isolated yield and 95.5:4.5 er. Reducing the chiral ligand to 5 mol

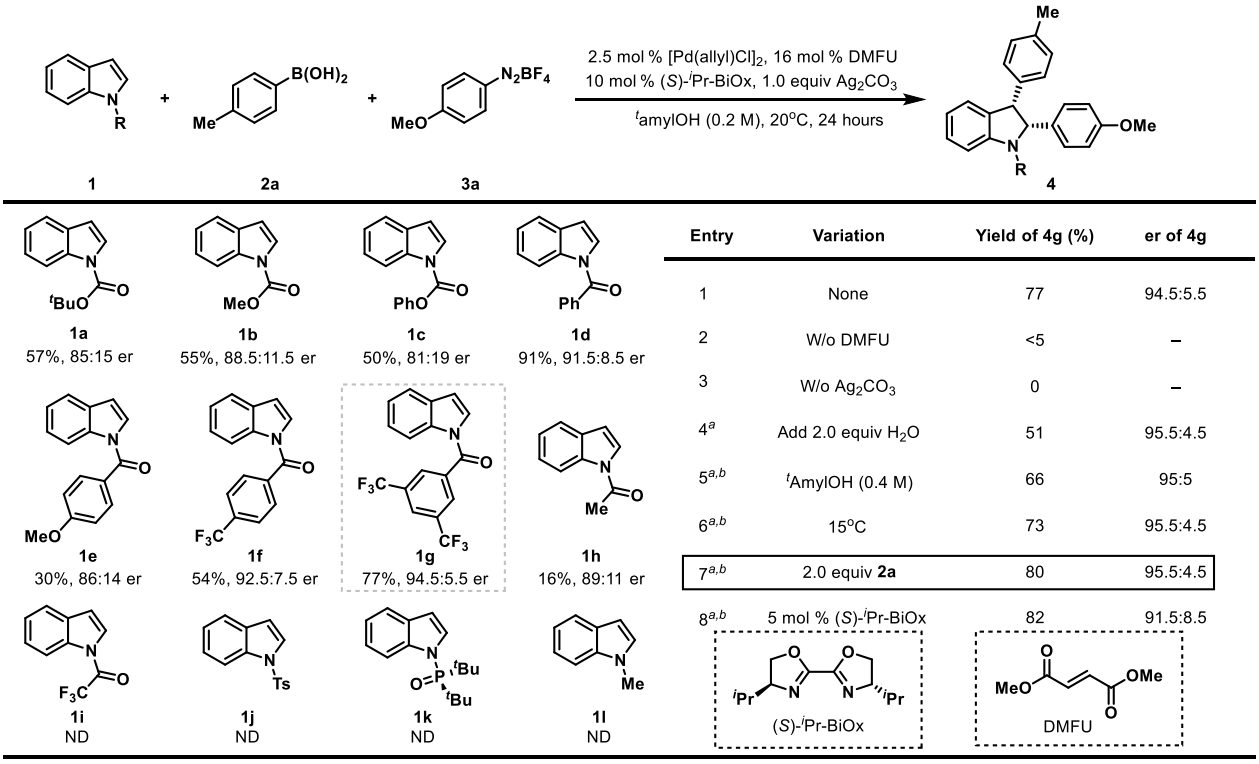

Fig. 2. Screening of reaction conditions. Reaction conditions: indole **1** (0.1 mmol), 4-$MeC_6H_4B(OH)_2$ **2a** (3.0 equiv, 0.30 mmol), 4-$MeOC_6H_4N_2BF_4$ **3a** (2.0 equiv, 0.20 mmol), $[Pd(allyl)Cl]_2$ (2.5 mol %, 0.0025 mmol), (*S*)-^{i}Pr-BiOx (10 mol %, 0.01 mmol), DMFU (16 mol %, 0.016 mmol), and Ag_2CO_3 (1.0 equiv, 0.1 mmol) in ^{t}amylOH (0.2 M, 0.5 ml) at 20°C for 24 hours. Isolated yields were reported, and the ers values were determined by chiral HPLC analysis. ND, no detection. [a]Ag_2CO_3 (2.0 equiv, 0.20 mmol). [b]H_2O (2.0 equiv, 0.20 mmol) was added.

% lowered the er (91.5:8.5). It should be noted that the potential C-2 or C-3 arylated indoles derived from the competitive C—H functionalization were not observed.

Substrate scopes

With optimized conditions established, we evaluated the generality of this asymmetric three-component dearomatization across diverse substrates (Fig. 3). For the nucleophilic coupling partners, arylboronic acids bearing para-electron-neutral or electron-withdrawing groups (**4m** to **4r**) delivered 2,3-diarylated indolines in good yields (56 to 91%) and enantioselectivities (94:6 to 96:4 er). Sensitive functionalities such as aldehydes (**4r**), halides (**4p**, **4s**, and **4t**), and nitro groups (**4u**) were well tolerated, offering handles for downstream derivatization. Sterically demanding 2-methoxyphenylboronic acid afforded **4v** in 61% yield and 95:5 er, whereas naphthyl (**4w**) and dibenzofuryl (**4x**) boronic acids provided products with retained stereocontrol. Electrophilic aryldiazonium salts with para- or meta-substituents (e.g., -Me, **4z** and **4ab**; -OMe, **4ac**; -Ph, **4aa**) performed robustly, yielding indolines with high enantioselectivity. Heteroatom-rich substrates, including 1,3-benzodioxole (**4ad**) and naphthalene (**4ae**), were compatible, although para-fluorinated diazonium salts (**4af**) exhibited reduced er (92.5:7.5). However, strong electron-withdrawing groups on the aryl diazonium salts, such as ester or nitrile functionalities, are not compatible under the standard conditions, likely due to the sluggish migratory insertion of electron-deficient Ar-Pd(II) species.

We further explored indole substrate scope (Fig. 4). Substituents at the C5 or C6 positions (-F, **4ag**; -Cl, **4ah**; -Me, **4ai**, **4aj**; -OMe, **4ak**) had minimal electronic impact, furnishing products in 51 to 80% yield and 93:7 to 95:5 er. However, a C7-methoxy group (**4al**) reduced yield (25%) due to steric disruption of the *N*-acyl-indole coplanarity. Notably, C2-methylated (**4am**) and *N*-methyl formate–protected indoles (**4an**) provided fully substituted carbons in moderate yield (38 to 40%) with good stereocontrol (90.5:9.5 to 93.5:6.5 er). Conversely, 2,3-dimethylated (**4ao**) or strongly electron-deficient indoles (e.g., -NO_2 and -CN) were unreactive, highlighting the method's sensitivity to steric and electronic perturbations.

Analogous to indoles, CADA of benzofurans offers a promising route to access stereochemically rich dihydrobenzofuran derivatives (*83*, *84*). Pleasingly, benzofuran **5a** proved compatible with our three-component dearomative cross-coupling protocol, regioselectively and diastereoselectively furnishing acyclic 2,3-diarylated dihydrobenzofuran **6a** in 67% yield and 93:7 er—marking the stereoselective synthesis of such scaffolds via benzofuran dearomatization (Fig. 5) (*85*). Ligand screening revealed that substituting (*S*)-^{i}Pr-BiOx with (*S*)-Cy-BiOx improved the yield (84%) but compromised enantiocontrol (87.5:12.5 er). X-ray crystallography confirmed **6a**'s absolute configuration. Bromo-substituted benzofurans delivered **6b** with enhanced yield and er using (*S*)-Cy-BiOx, whereas phenyl-substituted derivatives afforded **6c** with moderate efficiency. Notably, the protocol extended to the natural product xanthotoxin—a therapeutic agent for psoriasis, eczema, and related conditions (*86*)—yielding dearomatized **6d** in 64% yield

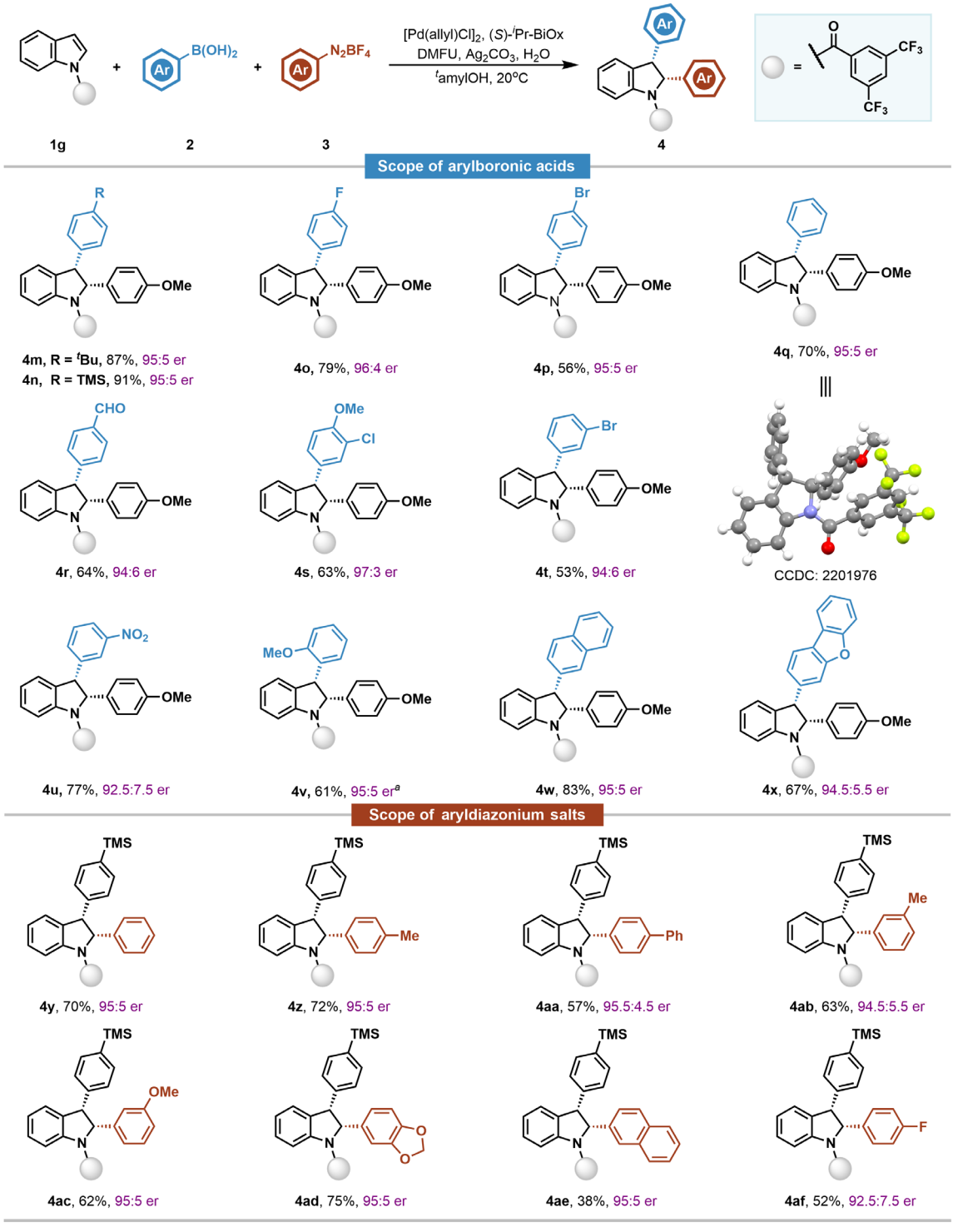

Fig. 3. Substrate scope of coupling component. The reaction was performed with indole (0.1 mmol), arylboronic acid (2.0 equiv, 0.2 mmol), aryldiazonium salt (2.0 equiv, 0.2 mmol), $[Pd(allyl)Cl]_2$ (2.5 mol %, 0.0025 mmol), (*S*)-^{i}Pr-BiOx (10 mol %, 0.01 mmol), DMFU (16 mol %, 0.016 mmol), Ag_2CO_3 (2.0 equiv, 0.2 mmol), and H_2O (2.0 equiv, 0.2 mmol) in ^{t}amylOH (0.2 M, 0.5 ml) at 20°C. Isolated yields were reported, and the ers were determined by chiral HPLC analysis. All reported data represent single runs. TMS, trimethylsilyl. [a]Arylboronic acid (3.0 equiv, 0.30 mmol), diphenyl fumarate instead of DMFU, Ag_2CO_3 (1.0 equiv, 0.10 mmol), and without H_2O.

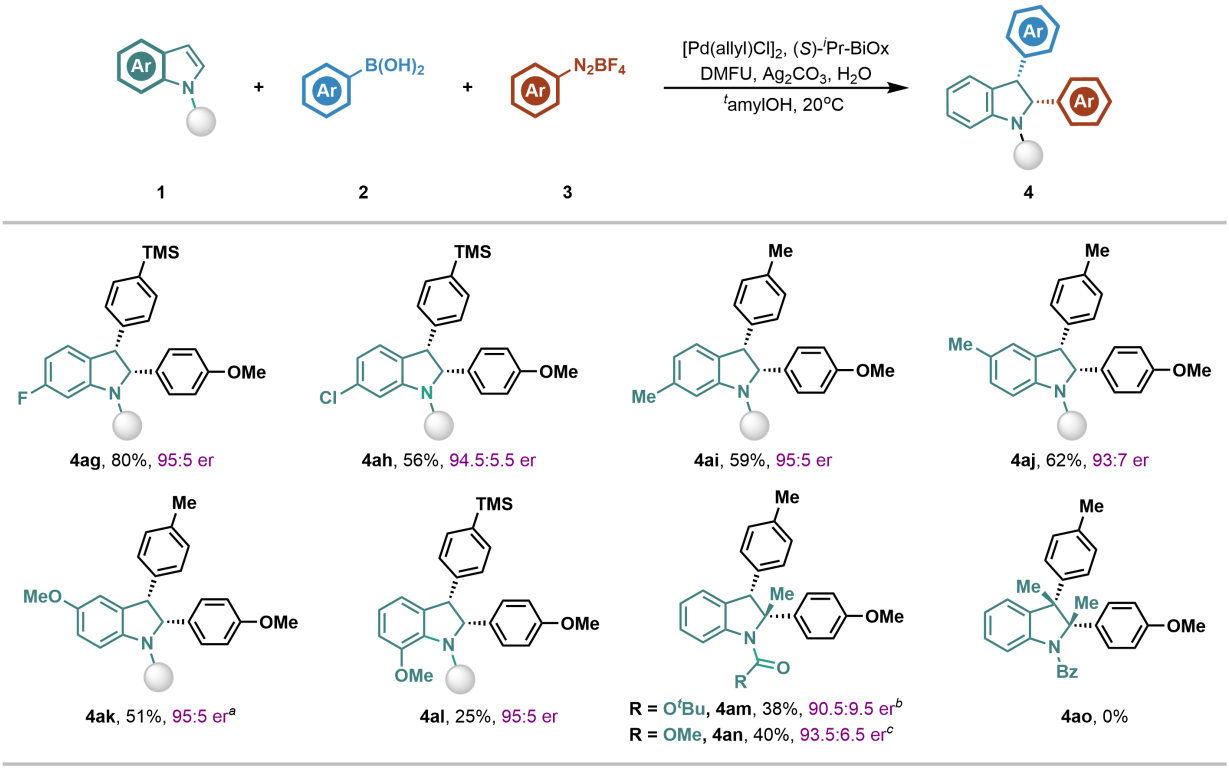

Fig. 4. Substrate scope of indoles. The reaction was performed with indole (0.1 mmol), arylboronic acid (2.0 equiv, 0.2 mmol), aryldiazonium salt (2.0 equiv, 0.2 mmol), $[Pd(allyl)Cl]_2$ (2.5 mol %, 0.0025 mmol), (*S*)-^{i}Pr-BiOx (10 mol %, 0.01 mmol), DMFU (16 mol %, 0.016 mmol), Ag_2CO_3 (2.0 equiv, 0.2 mmol), and H_2O (2.0 equiv, 0.2 mmol) in ^{t}amylOH (0.2 M, 0.5 ml) at 20°C. Isolated yields were reported, and the ers were determined by chiral HPLC analysis. All reported data represent single runs. [a]$Et_3N{\cdot}HBr$ (30 mol %) was added. [b]Arylboronic acid (3.0 equiv, 0.30 mmol), Ag_2CO_3 (1.0 equiv, 0.10 mmol), diphenyl fumarate instead of DMFU, and without H_2O. [c](*S*)-CyBiOx (10 mol %, 0.01 mmol) was used.

and 98.5:1.5 er, demonstrating applicability to complex, bioactive molecules. However, C2-substituted benzofuran **5e** and benzothiophene **5f** remained unreactive under current conditions, highlighting ongoing challenges in substrate scope.

To gain deeper insight into the reaction mechanism and the origins of enantioselectivity, we conducted density functional theory (DFT) calculations at the M06(SMD)/def2-TZVPP//B3LYP-D3(BJ)/SDD&6-31G(d) level of theory (see the Supplementary Materials for computational details). The experimentally used N-protected indole **1g**, arylboronic acid **2a**, and aryldiazonium cation **3a′** were selected as model substrates (Fig. 6A). Starting from **3a′**-Pd complex **IM1**, the C─N oxidative addition takes place via N_2 extrusion transition state **TS1**, requiring an energy barrier of only 2.7 kcal/mol relative to **IM1**. This step is highly exergonic, with resulting intermediate **IM2** being 35.1 kcal/mol more stable than **IM1**. Next, coordination of the C═C double bond of **1g** to the Pd center leads to more stable intermediate **IM3**, from which migratory insertion occurs via transition state **TS2**, yielding intermediate **IM4**. Subsequent transmetalation with **2a**-$AgCO_3$ proceeds through transition state **TS3**, resulting in the formation of $B(OH)_2$─$AgCO_3$ and intermediate **IM5**. The catalytic cycle is completed by C─C reductive elimination, which represents the rate-determining step of the overall reaction. However, the direct C─C reductive elimination from **IM5** via transition state **TS4** is kinetically challenging, with an energy barrier of 24.3 kcal/mol. Alternatively, although the formation of **IM6** through ligand exchange between **IM5** and DMFU is thermodynamically unfavorable, the subsequent C─C reductive elimination from **IM6** via transition state **TS5** is 7.8 kcal/mol lower in energy than **TS4** (−61.3 versus −69.1 kcal/mol). These findings are in accordance with the experimental results, underscoring the important role of DMFU in facilitating the reaction. This effect is likely due to the electron-poor nature of DMFU compared to (*S*)-^{i}Pr-BiOx, which renders the Pd center more electron-deficient and thereby promotes C─C reductive elimination. Last, ligand exchange between the resulting intermediate **IM7**, (*S*)-^{i}Pr-BiOx, and **3a′** delivers the final product **4g** and regenerates intermediate **IM1**.

The computations indicate that enantioselectivity is determined by the migratory insertion step. Specifically, transition state **TS2** is 1.8 kcal/mol lower in energy than **TS2′** (−33.3 versus −31.5 kcal/mol; Fig. 6B), aligning well with the experimentally observed enantioselectivity. The structural analysis shows that enantioselectivity primarily stems from steric repulsion between the N-protected indole and one of the isopropyl groups of (*S*)-^{i}Pr-BiOx. In **TS2**, the N-protected indole is predominantly located in the less hindered quadrant I, whereas in **TS2′**, it is mainly positioned in the more sterically congested quadrant IV. Consequently, steric repulsion between the N-protected indole and the isopropyl group makes **TS2′** higher in energy than **TS2**. On the basis of the literature reports and

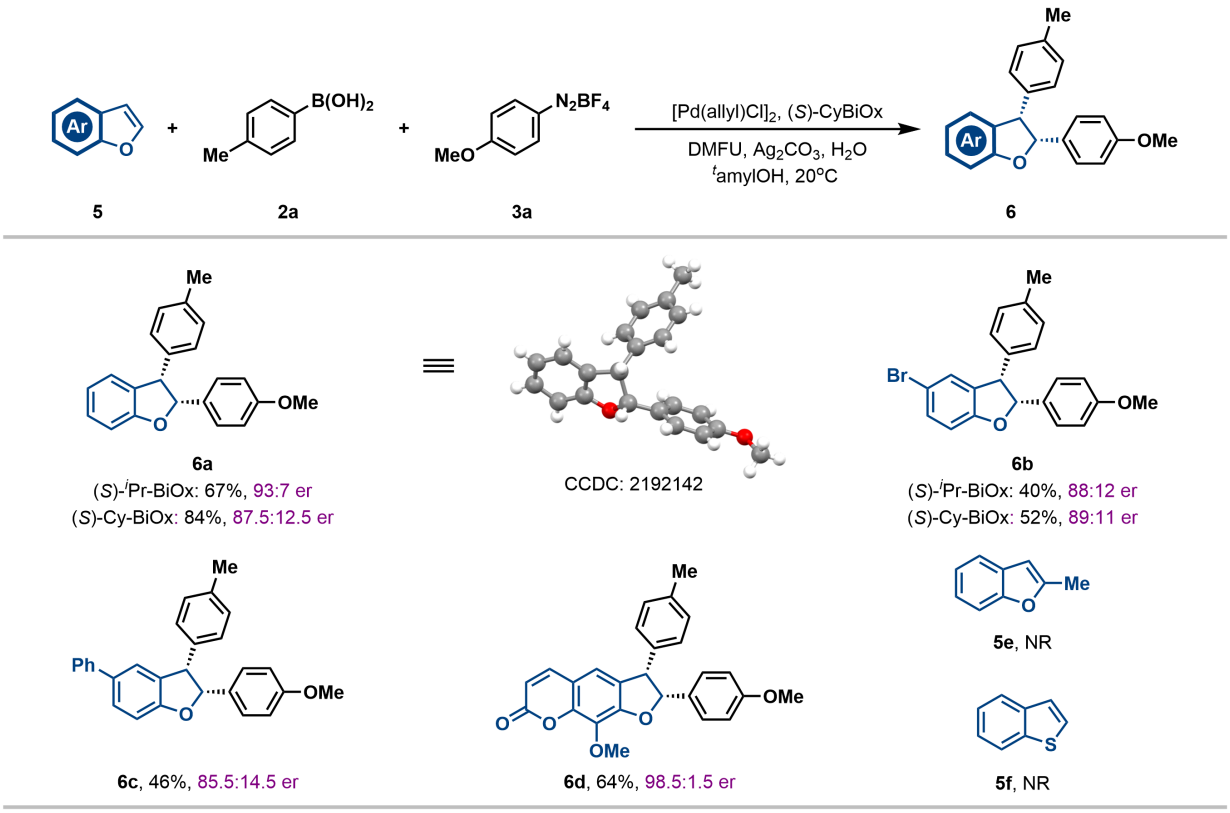

Fig. 5. Substrate scope of benzofurans. The reaction was performed with benzofuran **5** (0.1 mmol), 4-$MeC_6H_4B(OH)_2$ **2a** (2.0 equiv, 0.2 mmol), 4-$MeOC_6H_4N_2BF_4$ **3a** (2.0 equiv, 0.2 mmol), [Pd(allyl)Cl]2 (2.5 mol %, 0.0025 mmol), (*S*)-CyBiOx (10 mol %, 0.01 mmol), DMFU (16 mol %, 0.016 mmol), Ag_2CO_3 (2.0 equiv, 0.20 mmol), and H_2O (2.0 equiv, 0.2 mmol) in ^{t}amylOH (0.2 M, 0.5 ml) at 20°C. Isolated yields were reported, and the ers were determined by chiral HPLC analysis. All reported data represent single runs. NR, no reaction.

our mechanistic results (*62*, *80*–*82*), we propose the following plausible mechanism (Fig. 6C). The reaction was initiated with oxidative addition of Pd(0) catalyst, leading to aryl palladium(II) species **A**. Next, the aryl palladium(II) species underwent stereoselective migratory insertion with indole to deliver a chiral benzylic palladium intermediate **B**. We speculate that the stabilization of the benzylic palladium intermediate circumvents the undesired β-hydride elimination pathway. Subsequently, the arylboronic acid can intercept Pd species **B** in a transmetalation event to yield intermediate **C**, which would then undergo rapid ligand swap to yield intermediate **D**. The electron-deficient fumarate ligand could promote the reductive elimination to release the desired chiral indolines **4** and regenerate Pd(0) to close the cycle.

Treatment of **4g** with ^{n}BuLi at 0°C allows the cleavage of the *N*-3,5-bis(trifluoromethyl)phenyl-acyl group to deliver the corresponding N—H-containing 2,3-diarylated indoline **7** with maintaining the enantiomeric excess, which could potentially be carried for further transformations (Fig. 7).

In summary, we developed a palladium-catalyzed intermolecular asymmetric dearomatization of simple indoles and benzofurans via a three-component cross-coupling reaction with aryl diazonium salts and boronic acids. A ligand-swap strategy using a chiral BiOx ligand and an achiral fumarate ligand proved critical to achieving exceptional stereo-, regio-, and chemoselectivity. This method provides direct access to enantioenriched 2,3-diarylated indolines and dihydrobenzofurans bearing two contiguous stereocenters in moderate to excellent yields and enantioselectivities. Further exploration of the multicomponent asymmetric dearomative reaction of aromatic compounds and synthetic applications will be described in due course.

MATERIALS AND METHODS

General experimental procedures

Unless otherwise noted, materials were purchased from commercial suppliers and used without further purification. All catalytic reactions were carried out using oven-dried glassware and deoxygenated solvents under a dry nitrogen atmosphere. A glove box was used to handle extremely air-sensitive and moisture-sensitive reagents and reactions under a nitrogen atmosphere [oxygen and moisture levels were maintained at 0 to 2 parts per million (ppm) at all times]. ^{t}AmylOH was distilled over CaH_2; *N*,*N*′-dimethylformamide (DMF) (CAS 68-12-2) was purchased from Adamas [99.8%, SafeDry, water ≤ 50 ppm (by K.F.), SafeSeal]; $[Pd(allyl)Cl]_2$ was purchased from Sinocompound; DMFU (CAS 624-49-7) was purchased from D&B; Ag_2CO_3 (CAS 534-16-7) was purchased from Bidepharm. Reactions were monitored by thin-layer chromatography (TLC) carried out on 0.20-mm Huanghai silica gel plates (HSGF 254) using ultraviolet light as the visualizing agent and ceric ammonium molybdate solution (CAM) and an acidic solution of phosphomolybdic acid (PMA) with heat as the stains. All new compounds were characterized by means of ^{1}H nuclear magnetic resonance (NMR), ^{13}C NMR, ^{19}F NMR, and high-resolution mass spectrometry (HRMS). NMR spectra

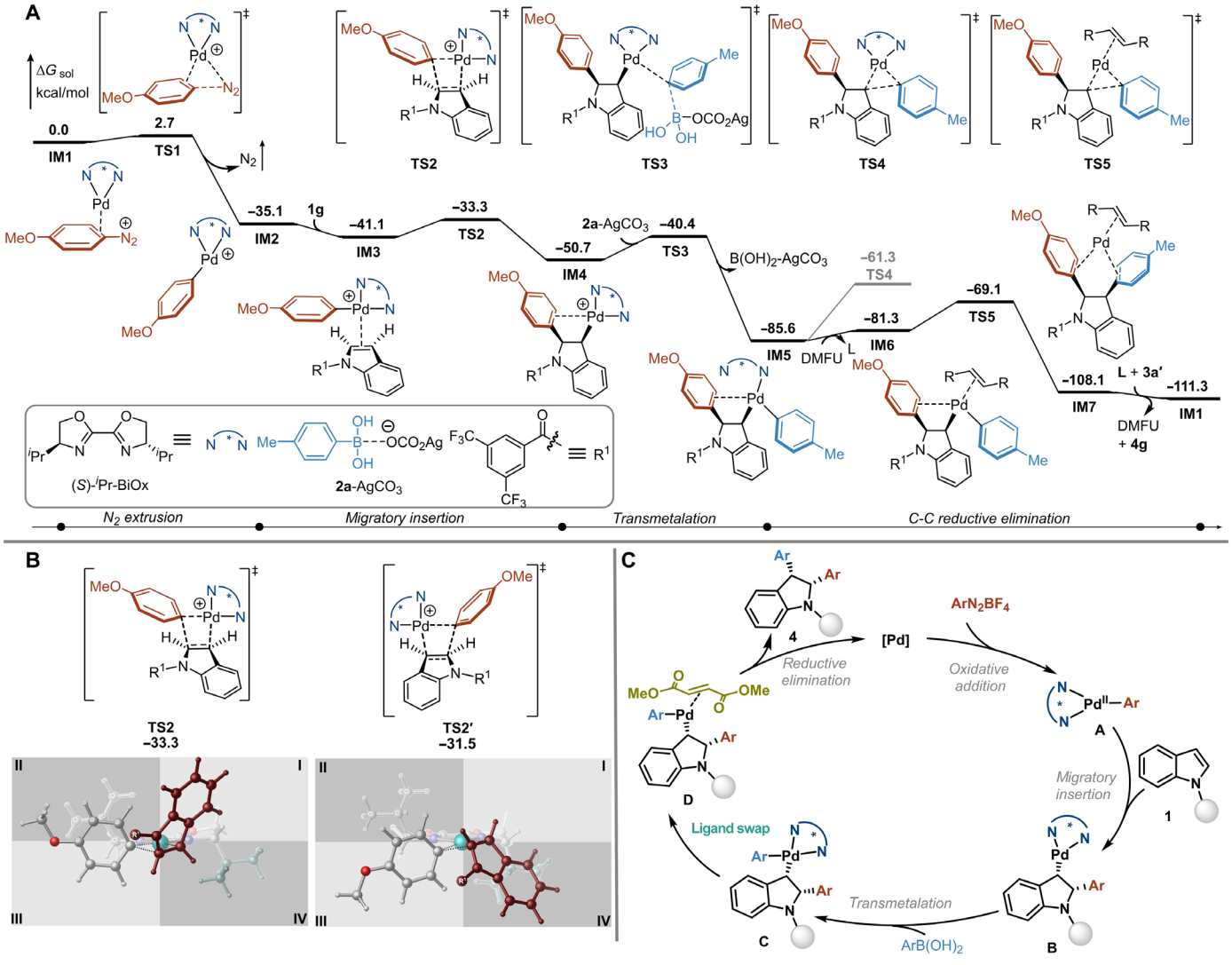

Fig. 6. Computational analysis. (**A**) Calculated energy profile of Pd-catalyzed diarylation of N-protected indole **1g**. (**B**) Optimized geometries and quadrant analysis of the migratory insertion transition states. Energies are given in kcal/mol. (**C**) Proposed mechanism.

Fig. 7. Cleavage of protecting group.

were recorded using a Bruker AVANCE III or Agilent 400-MHz NMR spectrometer and can be found at the end of the paper. High-resolution mass spectra were recorded on a Q Exactive plus 4G mass spectrometer using an ESI-Quadrupole-Orbitrap LC-MS. High-performance liquid chromatography (HPLC) was performed on a SHIMADZU LC-2030 Plus and SIL-20A. Optical rotations were recorded on digital automatic polarimeter (WZZ-2S). Melting points were obtained for all crystalline solids on an INESA SGW X-4 Melting-Point Apparatus with a microscope. Single-crystal x-ray diffraction data were collected at 293(2) K on a Bruker D8 Venture diffractometer. All ^{1}H NMR data are reported in δ units, ppm, and were calibrated relative to the signals for residual chloroform (7.26 ppm) in deuterochloroform ($CDCl_3$). All ^{13}C NMR data are reported in ppm relative to $CDCl_3$ (77.16 ppm). ^{19}F NMR was recorded on a Bruker AVANCE III 400 NMR spectrometer ($CFCl_3$ as an external standard and low field is positive), and data were obtained with ^{1}H decoupling.

General procedure for asymmetric 1,2-diarylation of indoles

To a dried sealed vial, $[Pd(allyl)Cl]_2$ (0.9 mg, 0.0025 mmol, 2.5 mol %), (*S*)-^{i}Pr-BiOx (2.2 mg, 0.01 mmol, 10 mol %), and DMFU (2.3 mg, 0.016 mmol, 16 mol %) were added. Then, arylboronic acid (0.2 mmol, 2.0 equiv), aryldiazonium salt (0.2 mmol, 2.0 equiv), Ag_2CO_3 (55.2 mg, 0.2 mmol, 2.0 equiv), and indole (0.1 mmol, 1.0 equiv) were subsequently added. The vial was transferred into a glove box, and H_2O (0.2 mmol, 2.0 equiv) and ^{t}amylOH (0.5 ml, 0.2 M) were added in sequence. The vial was then taken out from the glove box and stirred at 20°C. After the reaction was completed, the mixture was filtered through a short pad of silica gel with CH_2Cl_2 eluent and concentrated under reduced pressure by rotary evaporation. The desired product was purified by preparative TLC to provide the desired indolines.

Supplementary Materials

This PDF file includes:

Supplementary Text
Tables S1 to S10
Figs. S1 to S3
NMR Spectra
References

REFERENCES AND NOTES

1. E. Vitaku, D. T. Smith, J. T. Njardarson, Analysis of the structural diversity, substitution patterns, and frequency of nitrogen heterocycles among U.S. FDA approved pharmaceuticals. *J. Med. Chem.* **57**, 10257–10274 (2014).
2. T. V. Sravanthi, S. L. Manju, Indoles—A promising scaffold for drug development. *Eur. J. Pharm. Sci.* **91**, 1–10 (2016).
3. X.-Y. Liu, Y. Qin, Indole alkaloid synthesis facilitated by photoredox catalytic radical cascade reactions. *Acc. Chem. Res.* **52**, 1877–1891 (2019).
4. K. Urbina, D. Tresp, K. Sipps, M. Szostak, Recent advances in metal-catalyzed functionalization of indoles. *Adv. Synth. Catal.* **363**, 2723–2739 (2021).
5. Y.-C. Zhang, F. Jiang, F. Shi, Organocatalytic asymmetric synthesis of indole-based chiral heterocycles: Strategies, reactions, and outreach. *Acc. Chem. Res.* **53**, 425–446 (2020).
6. M. Bandini, A. Umani-Ronchi, *Catalytic Asymmetric Friedel–Crafts Alkylations* (Wiley-VCH, 2009).
7. A. Cerveri, M. Bandini, Recent advances in the catalytic functionalization of "electrophilic" Indoles. *Chin. J. Chem.* **38**, 287–294 (2020).
8. J. Wen, Z. Shi, From C4 to C7: Innovative strategies for site-selective functionalization of indole C–H bonds. *Acc. Chem. Res.* **54**, 1723–1736 (2021).
9. B. Prabagar, Y. Yang, Z. Shi, Site-selective C–H functionalization to access the arene backbone of indoles and quinolines. *Chem. Soc. Rev.* **50**, 11249–11269 (2021).
10. J. Szmuszkovicz, The reaction of 3-acylindoles with Grignard reagents. *J. Org. Chem.* **27**, 511–514 (1962).
11. C.-X. Zhuo, W. Zhang, S.-L. You, Catalytic asymmetric dearomatization reactions. *Angew. Chem. Int. Ed. Engl.* **51**, 12662–12686 (2012).
12. S.-L. You, *Asymmetric Dearomatization Reactions* (Wiley-VCH, 2016).
13. C. J. Huck, D. Sarlah, Shaping molecular landscapes: Recent advances, opportunities, and challenges in dearomatization. *Chem* **6**, 1589–1603 (2020).
14. W. Zi, Z. Zuo, D. Ma, Intramolecular dearomative oxidative coupling of indoles: A unified strategy for the total synthesis of indoline alkaloids. *Acc. Chem. Res.* **48**, 702–711 (2015).
15. J.-B. Chen, Y.-X. Jia, Recent progress in transition-metal-catalyzed enantioselective indole functionalizations. *Org. Biomol. Chem.* **15**, 3550–3567 (2017).
16. M.-Y. Teng, D.-Y. Liu, S.-Y. Mao, X. Wu, J.-H. Chen, M.-Y. Zhong, F. R. Huang, Q. J. Yao, B. F. Shi, Asymmetric dearomatization of indoles through cobalt-catalyzed enantioselective C–H functionalization enabled by photocatalysis. *Angew. Chem. Int. Ed. Engl.* **63**, e202407640 (2024).
17. A. Das, S. Kumaran, H. S. Ravi Sankar, J. R. Premkumar, B. Sundararaju, A dual cobalt-photoredox catalytic approach for asymmetric dearomatization of indoles with aryl amides via C–H activation. *Angew. Chem. Int. Ed. Engl.* **63**, e202406195 (2024).
18. Y. Xu, Y. Lin, S. L. Homölle, J. C. Oliveira, L. Ackermann, Enantioselective cobaltaphotoredox-catalyzed C–H activation. *J. Am. Chem. Soc.* **146**, 24105–24113 (2024).
19. X. Yu, C. Zheng, S.-L. You, Chiral Brønsted acid-catalyzed intramolecular asymmetric dearomatization reaction of indoles with cyclobutanones via cascade Friedel–Crafts/semipinacol rearrangement. *J. Am. Chem. Soc.* **146**, 25878–25887 (2024).
20. W. Fu, Y. Fu, Y. Zhao, H. Wang, P. Liu, Y. Yang, A metalloenzyme platform for catalytic asymmetric radical dearomatization. *Nat. Chem.* **16**, 1999–2008 (2024).
21. C. He, W. Song, D. Wei, W. Zhao, Q. Yu, J. Tang, Y. Ning, K. Murali, P. Sivaguru, G. de Ruiter, X. Bi, Rhodium-catalyzed asymmetric cyclopropanation of indoles with N-triftosylhydrazones. *Angew. Chem. Int. Ed. Engl.* **63**, e202408220 (2024).
22. X. Zhang, Q. Song, S. Liu, P. Sivaguru, Z. Liu, Y. Yang, Y. Ning, E. A. Anderson, G. de Ruiter, X. Bi, Asymmetric dearomative single-atom skeletal editing of indoles and pyrroles. *Nat. Chem.* **17**, 215–225 (2025).
23. Y.-Z. Liu, H. Song, C. Zheng, S.-L. You, Cascade asymmetric dearomative cyclization reactions via transition-metal-catalysis. *Nat. Synth.* **1**, 203–216 (2022).
24. G.-J. Mei, W. L. Koay, C. X. A. Tan, Y. Lu, Catalytic asymmetric preparation of pyrroloindolines: Strategies and applications to total synthesis. *Chem. Soc. Rev.* **50**, 5985–6012 (2021).
25. M. Pang, H. Chang, Z. Feng, J. Zhang, Recent advances in transition-metal-catalyzed tandem dearomatization of indoles. *Chin. J. Org. Chem.* **43**, 1271–1291 (2023).
26. X. Zhan, Z. Nie, N. Li, A. Zhou, H. Lv, M. Liang, K. Wu, G.-J. Cheng, Q. Yin, Catalytic asymmetric cascade dearomatization of indoles via a photoinduced Pd-catalyzed 1,2-bisfunctionalization of butadienes. *Angew. Chem. Int. Ed. Engl.* **63**, e202404388 (2024).
27. D.-S. Wang, Q.-A. Chen, S.-M. Lu, Y.-G. Zhou, Asymmetric hydrogenation of heteroarenes and arenes. *Chem. Rev.* **112**, 2557–2590 (2012).
28. A. N. Kim, B. M. Stoltz, Recent advances in homogeneous catalysts for the asymmetric hydrogenation of heteroarenes. *ACS Catal.* **10**, 13834–13851 (2020).
29. G. Liu, L. Zheng, K. Tian, H. Wang, L. W. Chung, X. Zhang, X.-Q. Dong, Ir-catalyzed asymmetric hydrogenation of unprotected indoles: Scope investigations and mechanistic studies. *J. Am. Chem. Soc.* **5**, 1398–1410 (2023).
30. K. Kubota, K. Hayama, H. Iwamoto, H. Ito, Enantioselective borylative dearomatization of indoles through copper(I) catalysis. *Angew. Chem. Int. Ed. Engl.* **54**, 8809–8813 (2015).
31. L. Chen, J.-J. Shen, Q. Gao, S. Xu, Synthesis of cyclic chiral α-amino boronates by copper-catalyzed asymmetric dearomative borylation of indoles. *Chem. Sci.* **9**, 5855–5859 (2018).
32. S. Panda, J. M. Ready, Palladium catalyzed asymmetric three-component coupling of boronic esters, indoles, and allylic acetates. *J. Am. Chem. Soc.* **139**, 6038–6041 (2017).
33. S. Panda, J. M. Ready, Tandem allylation/1,2-boronate rearrangement for the asymmetric synthesis of indolines with adjacent quaternary stereocenters. *J. Am. Chem. Soc.* **140**, 13242–13252 (2018).
34. S. Das, C. G. Daniliuc, A. Studer, Lewis acid catalyzed stereoselective dearomative coupling of indolylboron ate complexes with donor–acceptor cyclopropanes and alkyl halides. *Angew. Chem. Int. Ed. Engl.* **57**, 4053–4057 (2018).
35. A. K. Simlandy, M. K. Brown, Allenylidene induced 1,2-metalate rearrangement of indole-boronates: Diastereoselective access to highly substituted indolines. *Angew. Chem. Int. Ed. Engl.* **60**, 12366–12370 (2021).
36. R.-X. Liang, Y.-X. Jia, Aromatic π-components for enantioselective Heck reactions and Heck/anion-capture domino sequences. *Acc. Chem. Res.* **55**, 734–745 (2022).
37. N. Zeidan, M. Lautens, Migratory insertion strategies for dearomatization. *Synthesis* **51**, 4137–4146 (2019).
38. C. Shen, R.-R. Liu, R.-J. Fan, Y.-L. Li, T.-F. Xu, J.-R. Gao, Y.-X. Jia, Enantioselective arylative dearomatization of indoles via Pd-catalyzed intramolecular reductive Heck reactions. *J. Am. Chem. Soc.* **137**, 4936–4939 (2015).

39. K. Douki, H. Ono, T. Taniguchi, J. Shimokawa, M. Kitamura, T. Fukuyama, Enantioselective total synthesis of (+)-Hinckdentine A via a catalytic dearomatization approach. *J. Am. Chem. Soc.* **138**, 14578–14581 (2016).
40. R.-R. Liu, Y.-G. Wang, Y.-L. Li, B.-B. Huang, R.-X. Liang, Y.-X. Jia, Enantioselective dearomative difunctionalization of indoles by palladium-catalyzed Heck/Sonogashira sequence. *Angew. Chem. Int. Ed. Engl.* **56**, 7475–7478 (2017).
41. X. Qin, M. Wen, Y. Lee, J. Zhou, Nickel-catalyzed asymmetric reductive Heck cyclization of aryl halides to afford indolines. *Angew. Chem. Int. Ed. Engl.* **56**, 12723–12726 (2017).
42. C. Shen, N. Zeidan, Q. Wu, C. B. Breuers, R.-R. Liu, Y.-X. Jia, M. Lautens, Pd-catalyzed dearomative arylborylation of indoles. *Chem. Sci.* **10**, 3118–3122 (2019).
43. M.-L. Han, W. Huang, Y.-W. Liu, M. Liu, H. Xu, H. Xiong, H.-X. Dai, Pd-catalyzed asymmetric dearomatization of indoles via decarbonylative Heck-type reaction of thioesters. *Org. Lett.* **23**, 172–177 (2021).
44. Q. Li, Y. Zhang, Y. Zeng, Y. Fan, A. Lin, H. Yao, Palladium-catalyzed asymmetric dearomative carbonylation of indoles. *Org. Lett.* **24**, 3033–3037 (2022).
45. R.-X. Liang, J.-F. Chen, Y.-Y. Huang, Y.-P. Yu, H.-Y. Zhang, Y.-F. Song, C. G. Tsui, Y.-X. Jia, Enantioselective Pd-catalyzed dearomative reductive Heck and domino Heck–Suzuki reactions of 2-CF_3-indoles. *Chem. Commun.* **58**, 6200–6203 (2022).
46. B. Wang, J.-K. Gao, S. Sun, Z.-L. Shen, Y.-F. Yang, R.-X. Liang, Y.-X. Jia, Pd-catalyzed asymmetric intramolecular dearomatizing reductive Heck reaction of indoles. *Org. Lett.* **26**, 3739–3743 (2024).
47. X. Huang, M. Ou, L. Hong, W. Qin, Y. Ma, Diastereo- and enantioselective dearomative reductive aryl-fluoroalkenylation of indoles by nickel catalysis. *ACS Catal.* **14**, 6432–6439 (2024).
48. X. Li, B. Zhou, R.-Z. Yang, F.-M. Yang, R.-X. Liang, R.-R. Liu, Y.-X. Jia, Palladium-catalyzed enantioselective intramolecular dearomative Heck reaction. *J. Am. Chem. Soc.* **140**, 13945–13951 (2018).
49. R.-X. Liang, L.-J. Song, J.-B. Lu, W.-Y. Xu, C. Ding, Y.-X. Jia, Palladium-catalyzed enantioselective heteroarenyne cycloisomerization reaction. *Angew. Chem. Int. Ed. Engl.* **60**, 7412–7417 (2021).
50. D. Gao, L. Jiao, Divergent synthesis of indolenine and indoline ring systems by palladium-catalyzed asymmetric dearomatization of indoles. *Angew. Chem. Int. Ed. Engl.* **61**, e202116024 (2022).
51. H. Chu, J. Cheng, J. Yang, Y.-L. Guo, J. Zhang, Asymmetric dearomatization of indole by palladium/PC-phos-catalyzed dynamic kinetic transformation. *Angew. Chem. Int. Ed. Engl.* **59**, 21991–21996 (2020).
52. H.-F. Tu, X. Zhang, C. Zheng, M. Zhu, S.-L. You, Enantioselective dearomative prenylation of indole derivatives. *Nat. Catal.* **1**, 601–608 (2018).
53. P. Yang, R.-Q. Xu, C. Zheng, S.-L. You, Pd-catalyzed dearomatization of indole derivatives via intermolecular Heck reactions. *Chin. J. Chem.* **38**, 235–241 (2020).
54. S. Kirchberg, R. Fröhlich, A. Studer, Stereoselective palladium-catalyzed carboaminoxylations of indoles with arylboronic acids and TEMPO. *Angew. Chem. Int. Ed. Engl.* **48**, 4235–4238 (2009).
55. V. Ramella, Z. He, C. G. Daniliuc, A. Studer, Palladium-catalyzed diastereoselective oxyarylation of 2-alkylindoles. *Org. Lett.* **17**, 664–667 (2015).
56. Z. Liu, J. Chen, H.-X. Lu, X. Li, Y. Gao, R. J. Coombs, M. J. Goldfogel, K. M. Engle, Palladium(0)-catalyzed directed syn-1,2-carboboration and -silylation: Alkene scope, applications in dearomatization, and stereocontrol by a chiral auxiliary. *Angew. Chem. Int. Ed. Engl.* **58**, 17068–17073 (2019).
57. G. L. Trammel, R. Kuniyil, P. F. Crook, P. Liu, M. K. Brown, Nickel-catalyzed dearomative arylboration of indoles: Regioselective synthesis of C2- and C3-borylated indolines. *J. Am. Chem. Soc.* **143**, 16502–16511 (2021).
58. Z. Deng, L. Meng, X. Bing, S. Niu, X. Zhang, J. Peng, Y.-X. Luan, L. Chen, P.-P. Tang, Silver-enabled dearomative trifluoromethoxylation of indoles. *J. Am. Chem. Soc.* **146**, 2325–2332 (2024).
59. R. K. Dhungana, S. Kc, P. Basnet, R. Giri, Transition metal-catalyzed dicarbofunctionalization of unactivated olefins. *Chem. Rec.* **18**, 1314–1340 (2018).
60. Y. Ping, Y. Li, J. Zhu, W. Kong, Construction of quaternary stereocenters by palladium-catalyzed carbopalladation-initiated cascade reactions. *Angew. Chem. Int. Ed. Engl.* **58**, 1562–1573 (2019).
61. Y. Xi, W. Huang, C. Wang, H. Ding, T. Xia, L. Wu, K. Fang, J. Qu, Y. Chen, Catalytic asymmetric diarylation of internal acyclic styrenes and enamides. *J. Am. Chem. Soc.* **144**, 8389–8398 (2022).
62. W. Huang, Y. Xi, D. Pan, L. Fan, K. Fang, G. Huang, W.-H. Zhu, J. Qu, Y. Chen, Palladium-catalyzed enantioselective multicomponent cross-coupling of trisubstituted olefins. *J. Am. Chem. Soc.* **146**, 16892–16901 (2024).
63. O. Apolinar, T. Kang, T. M. Alturaifi, P. G. Bedekar, C. Z. Rubel, J. Derosa, B. B. Sanchez, Q. N. Wong, E. J. Sturgell, J. S. Chen, S. R. Wisniewski, P. Liu, K. M. Engle, Three-component asymmetric Ni-catalyzed 1,2-dicarbofunctionalization of unactivated alkenes via stereoselective migratory insertion. *J. Am. Chem. Soc.* **144**, 19337–19343 (2022).
64. Z. Dong, Q. Tang, C. Xu, L. Chen, H. Ji, S. Zhou, L. Song, L.-A. Chen, Directed asymmetric nickel-catalyzed reductive 1,2-diarylation of electronically unactivated alkenes. *Angew. Chem. Int. Ed. Engl.* **62**, e202218286 (2023).
65. X. Wu, B. Luan, W. Zhao, F. He, X.-Y. Wu, J. Qu, Y. Chen, Catalytic desymmetric dicarbofunctionalization of unactivated alkenes. *Angew. Chem. Int. Ed. Engl.* **61**, e202111598 (2022).
66. X. Wu, A. Turlik, B. Luan, F. He, J. Qu, K. N. Houk, Y. Chen, Nickel-catalyzed enantioselective reductive alkyl-carbamoylation of internal alkenes. *Angew. Chem. Int. Ed. Engl.* **61**, e202207536 (2022).
67. X. Wu, J. Qu, Y. Chen, Quinim: A new ligand scaffold enables nickel-catalyzed enantioselective synthesis of α-alkylated γ-lactam. *J. Am. Chem. Soc.* **142**, 15654–15660 (2020).
68. Y. Xi, Y. Chen, Recent advances in transition metal-catalyzed asymmetric functionalization of enamides. *Synthesis* **55**, 4464–4660 (2022).
69. B. Ju, S. Chen, W. Kong, Enantioselective palladium-catalyzed diarylation of unactivated alkenes. *Chem. Commun.* **55**, 14311–14314 (2019).
70. Z. Wang, J. Zhu, M. Wang, P. Lu, Palladium-catalyzed divergent enantioselective functionalization of cyclobutenes. *J. Am. Chem. Soc.* **146**, 12691–12701 (2024).
71. Z.-M. Zhang, B. Xu, L. Wu, Y. Wu, Y. Qian, L. Zhou, Y. Liu, J. Zhang, Enantioselective dicarbofunctionalization of unactivated alkenes by palladium-catalyzed tandem Heck/Suzuki coupling reaction. *Angew. Chem. Int. Ed. Engl.* **58**, 14653–14659 (2019).
72. D. Anthony, Q. Lin, J. Baudet, T. Diao, Nickel-catalyzed asymmetric reductive diarylation of vinylarenes. *Angew. Chem. Int. Ed. Engl.* **58**, 3198–3202 (2019).
73. S.-D. Yang, C.-L. Sun, Z. Feng, B.-J. Li, Y.-Z. Li, Z.-J. Shi, Palladium-catalyzed direct arylation of (hetero)arenes with aryl boronic acids. *Angew. Chem. Int. Ed. Engl.* **47**, 1473–1476 (2008).
74. H. P. L. Gemoets, I. Kalvet, A. V. Nyuchev, N. Erdmann, V. Hessel, F. Schoenebeck, T. Noël, Mild and selective base-free C–H arylation of heteroarenes: Experiment and computation. *Chem. Sci.* **8**, 1046–1055 (2017).
75. D. R. Stuart, K. Fagnou, The catalytic cross-coupling of unactivated arenes. *Science* **316**, 1172–1175 (2007).
76. Z.-X. Wang, X.-Y. Bai, B.-J. Li, Metal-catalyzed substrate-directed enantioselective functionalization of unactivated alkenes. *Chin. J. Chem.* **37**, 1174–1180 (2019).
77. Y. Yang, X. Qiu, Y. Zhao, Y. Mu, Z. Shi, Palladium-catalyzed C–H arylation of indoles at the C7 position. *J. Am. Chem. Soc.* **138**, 495–498 (2016).
78. Y. Wang, Y. He, S. Zhu, Nickel-catalyzed migratory cross-coupling reactions: New opportunities for selective C–H functionalization. *Acc. Chem. Res.* **56**, 3475–3491 (2023).
79. Y. Sun, B. Wang, Z. Lu, Ligand relay catalysis: A newly emerged synthetic strategy. *Org. Chem. Front.* **10**, 4146–4160 (2023).
80. J. B. Johnson, T. Rovis, More than bystanders: The effect of olefins on transition-metal-catalyzed cross-coupling reactions. *Angew. Chem. Int. Ed. Engl.* **47**, 840–871 (2008).
81. V. Aryal, L. J. Chesley, D. Niroula, R. R. Sapkota, R. K. Dhungana, R. Giri, Ni-catalyzed regio- and stereoselective alkylarylation of unactivated alkenes in γ,δ-alkenylketimines. *ACS Catal.* **12**, 7262–7268 (2022).
82. J. Derosa, R. Kleinmans, V. T. Tran, M. K. Karunananda, S. R. Wisniewski, M. D. Eastgate, K. M. Engle, Nickel-catalyzed 1,2-diarylation of simple alkenyl amides. *J. Am. Chem. Soc.* **140**, 17878–17883 (2018).
83. Q. Cheng, H.-J. Zhang, W.-J. Yue, S.-L. You, Palladium-catalyzed highly stereoselective dearomative [3+2] cycloaddition of nitrobenzofurans. *Chem* **3**, 428–436 (2017).
84. H. Wang, J. Zhang, Y. Tu, J. Zhang, Phosphine-catalyzed enantioselective dearomative [3+2]-cycloaddition of 3-nitroindoles and 2-nitrobenzofurans. *Angew. Chem. Int. Ed. Engl.* **58**, 5422–5426 (2019).
85. X. Yu, Q.-Y. Meng, C. G. Daniliuc, A. Studer, Aroyl fluorides as bifunctional reagents for dearomatizing fluoroaroylation of benzofurans. *J. Am. Chem. Soc.* **144**, 7072–7079 (2022).
86. B.-L. Zhang, C.-Q. Fan, L. Dong, F.-D. Wang, J.-M. Yue, Structural modification of a specific antimicrobial lead against helicobacter pylori discovered from traditional chinese medicine and a structure–activity relationship study. *Eur. J. Med. Chem.* **45**, 5258–5264 (2010).
87. X. S. Ning, X. Liang, K. F. Hu, C. Z. Yao, J. P. Qu, Y. B. Kang, Pd-^{t}BuONO cocatalyzed aerobic indole synthesis. *Adv. Synth. Catal.* **360**, 1590–1594 (2018).
88. X.-Y. Zhou, X. Chen, An easy-to-operate *N*-carbonylation of indoles with diaryl carbonates as reagent and Na_2CO_3 as catalyst. *Synth. Commun.* **50**, 1854–1862 (2020).
89. Q. Han, S. Fu, X. Zhang, S. Lin, Q. Huang, Facile approaches toward the synthesis of 6H-isoindolo[2,1-α]indol-6-ones via palladium-catalyzed carbonylation with carbon monoxide. *Tetrahedron Lett.* **57**, 4165–4169 (2016).
90. L. Wang, H. Neumann, A. Spannenberg, M. Beller, An efficient protocol to synthesize *N*-acyl-enamides and -imines by Pd-catalyzed carbonylations. *Chem. Eur. J.* **24**, 2164–2172 (2018).
91. Y. Ito, S. Nakatani, R. Shiraki, T. Kodama, M. Tobisu, Nickel-catalyzed addition of C-C bonds of amides to strained alkenes: The 1,2-carboaminocarbonylation reaction. *J. Am. Chem. Soc.* **144**, 662–666 (2022).

92. G. Ozuduru, T. Schubach, M. M. Boysen, Enantioselective cyclopropanation of indoles: Construction of all-carbon quaternary stereocenters. *Org. Lett.* **14**, 4990–4993 (2012).
93. J. E. Nordlander, D. B. Catalane, K. D. Kotian, R. M. Stevens, J. E. Haky, Synthesis of indoles from N-(trifluoroacetyl)-2-anilino acetals. *J. Org. Chem.* **46**, 778–782 (1981).
94. J. Cao, Z.-L. Chen, S.-M. Li, G.-F. Zhu, Y.-Y. Yang, C. Wang, W.-Z. Chen, J.-T. Wang, J.-Q. Zhang, L. Tang, Palladium-catalyzed regioselective C-2 arylation of benzofurans with *N′*-acyl arylhydrazines. *Eur. J. Org. Chem.* **2018**, 2774–2779 (2018).
95. M. J. Frisch, G. W. Trucks, J. Schlegel, G. E. Scuseria, M. A. Robb, J. R. Cheeseman, H. B. Schlegel, G. Scalmani, V. Barone, B. Mennucci, G. A. Petersson, Gaussian 09, Revision E.01 (Gaussian Inc., 2013).
96. J. Tao, J. P. Perdew, V. N. Staroverov, G. E. Scuseria, Climbing the density functional ladder: Nonempirical meta–generalized gradient approximation designed for molecules and solids. *Phys. Rev. Lett.* **91**, 146401 (2003).
97. E. Caldeweyher, C. Bannwarth, S. Grimme, Extension of the D3 dispersion coefficient model. *J. Chem. Phys.* **147**, 034112 (2017).
98. F. Weigend, R. Ahlrichs, Balanced basis sets of split valence, triple zeta valence and quadruple zeta valence quality for H to Rn: Design and assessment of accuracy. *Phys. Chem. Chem. Phys.* **7**, 3297–3305 (2005).
99. K. Fukui, Formulation of the reaction coordinate. *J. Phys. Chem.* **74**, 4161–4163 (1970).
100. K. Fukui, The path of chemical reactions—The IRC approach. *Acc. Chem. Res.* **14**, 363–368 (1981).
101. S. Grimme, C. Bannwarth, P. Shushkov, A robust and accurate tight-binding quantum chemical method for structures, vibrational frequencies, and noncovalent interactions of large molecular systems parametrized for all spd-block elements (Z = 1–86). *J. Chem. Theory Comput.* **13**, 1989–2009 (2017).
102. Y. Zhao, D. G. Truhlar, Density functionals with broad applicability in chemistry. *Acc. Chem. Res.* **41**, 157–167 (2008).
103. Y. Zhao, D. G. Truhlar, The M06 suite of density functionals for main group thermochemistry, thermochemical kinetics, noncovalent interactions, excited states, and transition elements: Two new functionals and systematic testing of four M06-class functionals and 12 other functionals. *Theor. Chem. Acc.* **120**, 215–241 (2008).
104. A. V. Marenich, C. J. Cramer, D. G. Truhlar, Universal solvation model based on solute electron density and on a continuum model of the solvent defined by the bulk dielectric constant and atomic surface tensions. *J. Phys. Chem. B* **113**, 6378–6396 (2009).
105. T. Lu, F. Chen, Multiwfn: A multifunctional wavefunction analyzer. *J. Comput. Chem.* **33**, 580–592 (2012).

Acknowledgments
Funding: This work was supported by the Key Project of Science and Technology Innovation 2030 (no. 2023ZD0121002), the National Natural Science Foundation of China (22171079, 22371071, 92356301, T2488302, 22073066, and 22471191), Science and Technology Commission of Shanghai Municipality (grant no. 24DX1400200), the Program of Introducing Talents of Discipline to Universities (B16017), Scientific Committee of Shanghai (21JC1401700), the China Postdoctoral Science Foundation (2023TQ0118), Postdoctoral Fellowship Program of CPSF (GZB20230212), and the Fundamental Research Funds for the Central Universities. We thank the Analysis and Testing Center of East China University of Science and Technology for help with NMR and HRMS analysis. **Author contributions:** Y.X. and Y.C. conceptualized the projects. Y.X., L.F., C.W., and T.X. performed the experiments under the supervision of J.Q. and Y.C. Y.-Z. X. conducted the DFT calculations under the supervision of G.H. Y.X., G.H., and Y.C. wrote the manuscript with the feedback of all other authors. **Competing interests:** The authors declare that they have no competing interests. **Data and materials availability:** All data needed to evaluate the conclusions in the paper are present in the paper and/or the Supplementary Materials.

Submitted 2 February 2025
Accepted 24 April 2025
Published 30 May 2025
10.1126/sciadv.adw4471